Ultra-wide frequency broadening mechanism for micro-scale electromagnetic energy harvester

Huicong Liu, Kah How Koh, and Chengkuo Lee

Citation: Applied Physics Letters **104**, 053901 (2014); doi: 10.1063/1.4863565
View online: http://dx.doi.org/10.1063/1.4863565
View Table of Contents: http://scitation.aip.org/content/aip/journal/apl/104/5?ver=pdfcov
Published by the AIP Publishing

APPLIED PHYSICS LETTERS **104**, 053901 (2014)

Ultra-wide frequency broadening mechanism for micro-scale electromagnetic energy harvester

Huicong Liu,[1,2] Kah How Koh,[2] and Chengkuo Lee[2,a)]
[1]*Robotics and Microsystems Center & Collaborative Innovation Center of Suzhou Nano Science and Technology, Soochow University, Suzhou 215021, People's Republic of China*
[2]*Department of Electrical and Computer Engineering, National University of Singapore, 9 Engineering Drive 1, Singapore 117576*

(Received 22 November 2013; accepted 12 January 2014; published online 3 February 2014)

This work proposed a hybrid frequency broadening (HFB) mechanism in micro-scale for vibration energy harvesting with ultra-wide bandwidth. A strong HFB behavior is induced by the Duffing stiffening of the clamped-clamped beam stretching and further stimulated continuously by three distributed resonances including out-of-plane mode I at 62.9 Hz, torsion mode II at 82.1 Hz, and twist mode III at 150 Hz. At the acceleration of 1.0g, the microfabricated device with a small area of $6 \times 6\,\text{mm}^2$ is able to broaden the operating bandwidth from 62.9 Hz to be as wide as 383.7 Hz. This design methodology can be implemented for efficient electromagnetic energy harvesting. [http://dx.doi.org/10.1063/1.4863565]

At present, harvesting vibration energy from the environment is an attractive alternative power source for low-power wireless sensing applications.[1] Various frequency broadening strategies[2] for vibrational energy harvesting have been reported to overcome the narrow operating bandwidth of traditional linear harvester systems, in which the output power drop dramatically under off-resonance conditions. The recent attempts through the use of nonlinear or multi-frequency oscillation structures have improved the operating frequency range to a certain extent, but not in significant. Nevertheless, few of them are feasible for micro-machining process. Liu *et al.*[3,4] have employed an end-stop mechanism to achieve piecewise linear spring stiffness and hence gained wide bandwidth of a micro-electro-mechanical-systems (MEMSs) piezoelectric harvester while at the cost of suppressed vibration amplitude and power output. Tvedt *et al.*[5] and Nguyen *et al.*[6] have achieved the bandwidth enhancement of nonlinear electrostatic MEMS harvesters via purely beam-spring geometrical design. However, they require extra high bias voltages. Recently, an effective nonlinear concept of stretching strain was reported to induce significant nonlinearity for ultra-wide bandwidth harvesting.[7,8] In the meantime, multi-frequency energy harvesting concept, which is an alternative solution of continuous wideband frequency response, has been reported to gain multiple discrete frequency spectra along a certain frequency range.[9–11] None of previous works have made the attempt of combination of both frequency broadening solutions. In this work, the authors present the attempt of hybrid of both nonlinear and multi-frequency harvesting mechanisms so as to realize an ultra-wide operating bandwidth. The prototype is micromachined and assembled with permanent magnet to demonstrate an electromagnetic (EM) induced energy harvesting capability.

Figure 1(a) indicates a schematic drawing of the proposed hybrid frequency broadening (HFB) mechanism for EM energy harvesting. Instead of using a common free-end cantilever beam, the design contains a pair of thin clamped-clamped beams and a large mass frame connected through the middle beam joints. The mass frame is integrated with reflective surface in the center for monitoring its vibration behavior via light reflection approach. The EM coils of 5 μm in width and 5 μm in spacing are wounded to the bonding pads at the outer frame. The design is microfabricated with a frame size of 6 mm × 6 mm × 0.4 mm as shown in Fig. 1(b). Each clamped beam has an equal beam length of 1.9 mm, width of 0.2 mm, and thickness of 5 μm. Each beam joint is 1.2 mm in length, 0.2 mm in width, and 0.4 mm in thickness. The mass frame has a dimension of 4.6 mm in length, 2.9 mm in width, and 0.4 mm in thickness. A cylindrical magnet of 6 mm in diameter is placed on top of the chip frame with a gap distance of 2 mm, such that a uniform magnetic field of flux density $\vec{B}$ is introduced across the mass frame (z-direction). Hence, the electric current will be generated in the EM coils through the vibration of the mass frame. The energy harvesting chip is micro-fabricated on a silicon-on-insulator wafer and its cross-sectional view along A-A′ is shown in Fig. 1(c). Fig. 1(d) shows an optical image of the released chip.

As the mass frame experiences a large deflection, it will induce strain to the thin clamped-clamped beams in two forms: Bending strain δ_b and stretching strain δ_s ($\delta = \delta_b + \delta_s$). The force-deflection characteristic can be modeled as an amplitude-stiffened Duffing spring and is expressed as[12]

$$F = \left(\frac{\pi^4}{6}\right)\left[\frac{Ewh^3}{l^3}\right]x + \left(\frac{\pi^4}{8}\right)\left[\frac{Ewh}{l^3}\right]x^3, \tag{1}$$

where F is the equivalent concentrated force applied to the center of the clamped-clamped beam; E is the Young's modulus of the beam material; w, h, and l are the width, thickness, and length of the clamped-clamped beam, respectively. In Eq. (1), the first linear term due to the beam bending strain is proportional to the moment of inertia (i.e., wh^3). The

a)Author to whom correspondence should be addressed. Electronic mail: elelc@nus.edu.sg. Tel.: (65)6516-5865. FAX: (65)6779-1103

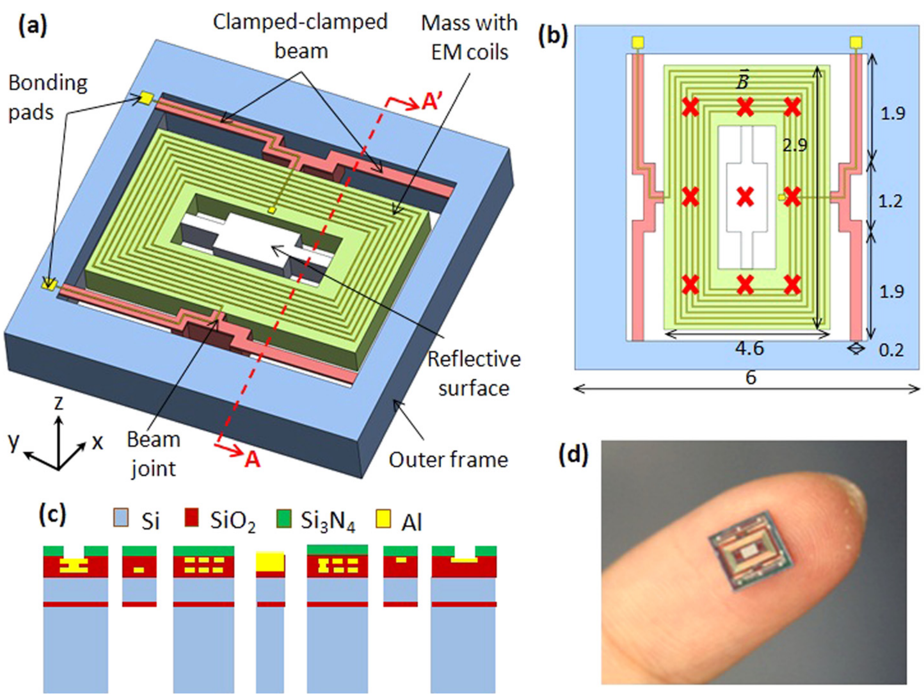

FIG. 1. (a) Schematic illustration, (b) top view, and (c) cross-sectional view along A-A′ of a HFB mechanism for EM energy harvesting; (d) an optical image of the released chip.

second nonlinear term (x^3) introduced by the stretching strain is proportional in terms of wh. As can be seen, a thicker beam will be more likely dominated by the bending term, while the stretching term will play a dominant role in a thinner beam. Furthermore, the transition from the bending-dominated linear behavior to stretching-dominated nonlinear behavior occurs when the displacement x is larger than the beam thickness h. The strong nonliearity of the structure will enable the wide operating bandwidth of the system.

The mode analysis is essentially to establish the modal model and conduct the numerical analysis. Since the structural damping has little effect on the modal frequency and vibration shape, the modal vector of the equation of motion can be solved by a finite number of degrees of freedom without damping and external load. The matrix equation of an undamped free vibration system can be expressed as

$$[M]\{\ddot{u}\} + [K]\{u\} = \{0\}, \tag{2}$$

where $[M]$ is the mass matrix, $[K]$ is the stiffness matrix, $\{u\}$ is the displacement ($u(t) = \phi_n \exp(i\omega_n t)$), and $\{\ddot{u}\}$ is the 2nd time derivative of the displacement (i.e., the acceleration). Equation (2) is the general form of the eigensystem encountered using finite element modeling. To describe the solutions of the free vibration system, $\{\ddot{u}\}$ is taken to equal $-\lambda\{u\}$, where λ is the eigenvalues ($\lambda = \omega_n^2$). Hence, Eq. (2) is reduced to

$$[K - \lambda M]\{\varphi_n\} = \{0\}. \tag{3}$$

The condition for non-zero solutions of $\{u\}$ is $|K - \lambda M| = 0$. Subsequently, the disperse roots of λ_i ($i = 1, 2, \ldots$ n) can be solved, and $\{\phi_{ni}\}$ is the corresponding ith eigenvector. In this study, the vibration behavior of the HFB design is studied by finite element analysis (FEA) using commercial software Abaqus. In the simulation, the material properties of silicon have Young's modulus of 169 GPa and density of 2.33×10^3 kg/cm^3. Figure 2 shows the natural frequencies

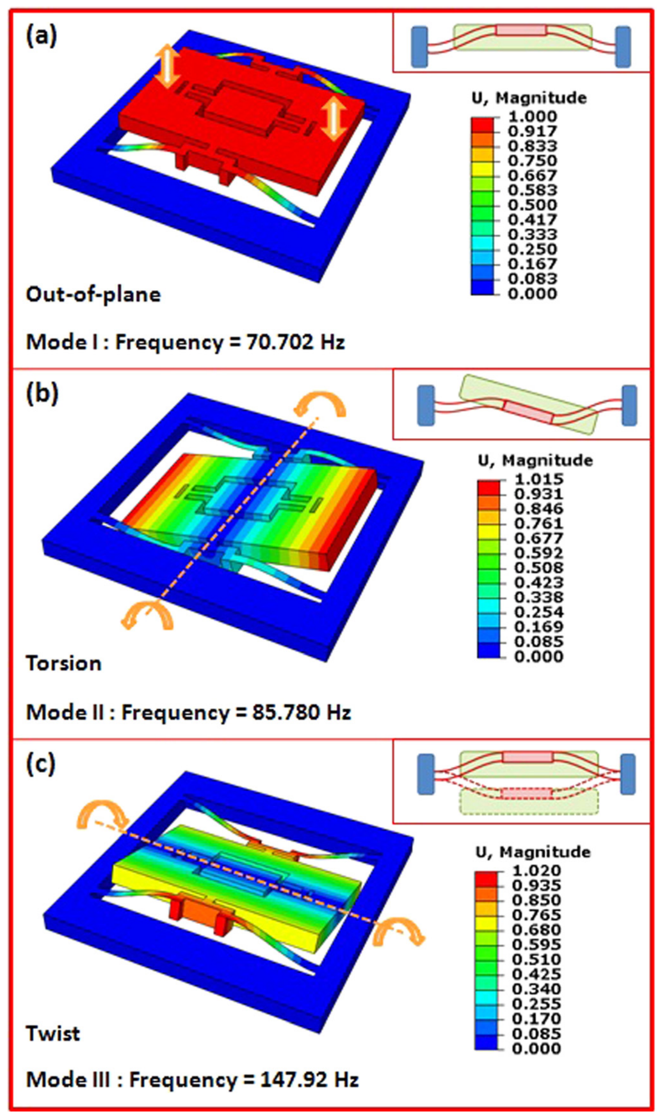

FIG. 2. Finite element analysis of the first three mode shapes: (a) mode I at 70.7 Hz; (b) mode II at 85.7 Hz; and (c) mode III at 147.9 Hz.

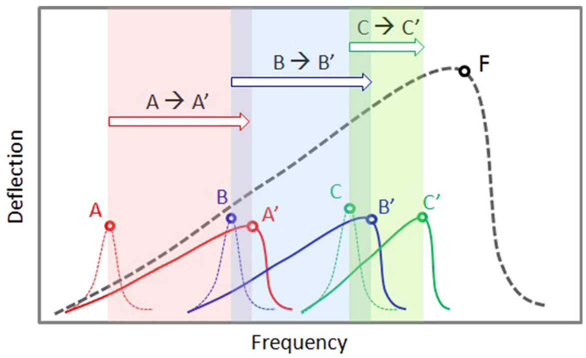

FIG. 3. Illustration of the working principle for HFB mechanism.

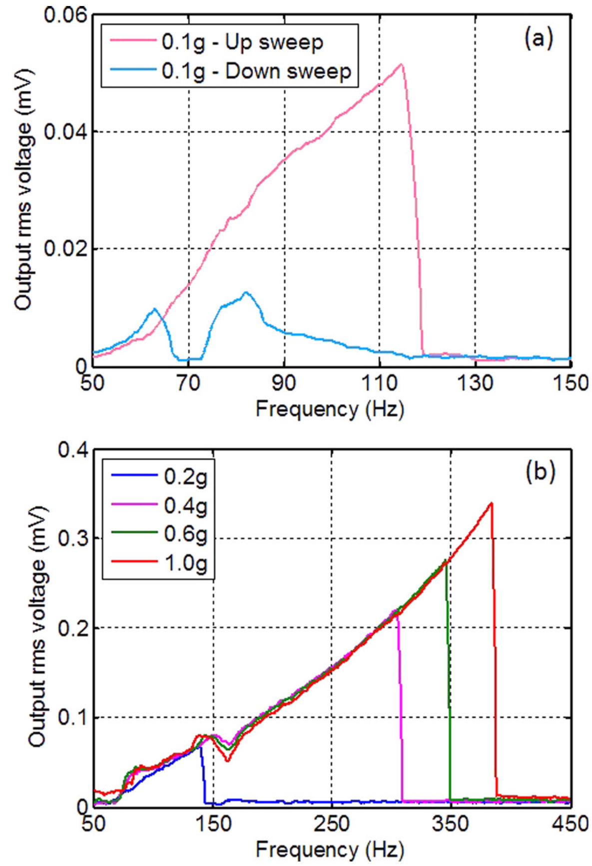

FIG. 4. Experimental results of (a) the output voltages against frequency up-sweep and down-sweep at a low acceleration of 0.1g; (b) the output voltage against frequency up-sweep at accelerations of 0.2g, 0.4g, 0.6g, and 1.0g.

and mode shapes of the first three modes of the HFB structure, which are out-of-plane mode (mode I) at 70.7 Hz, torsion mode (mode II) at 85.8 Hz, and twist mode (mode III) at 147.9 Hz. The inset figure of each mode at its top-right corner shows the section diagram of the deflection of the clamped-clamped beam. It is obvious that the out-of-plane, torsion and twist vibrations at the three resonance modes result in large beam deflection and stretching strain, which will lead to nonlinear response at each mode. In the case that the three original resonances are close to each other, the low-order resonance due to nonlinear effect would engage its neighboring high-order resonance. Such interaction will enhance the nonlinearity and eventually gain a continuous frequency broadening effect towards an ultra-wide bandwidth.

To be more specific, the working principle of HFB mechanism is illustrated in Fig. 3, by assuming that the three original resonant frequencies at points A, B, and C are close to each other. Due to the stretching strain of the clamped-clamped beams, the out-of-plane mode I, torsion mode II, and twist mode III show strong nonlinearity and could broaden each individual resonance towards points A′, B′, and C′, respectively. Since the nonlinear resonance at mode I is large enough, such that it exceeds the adjacent resonance II, i.e., $A' > B$, the nonlinear response will be further enhanced from point B towards an even wider frequency. Similarly, once this further strengthened nonlinear resonance is larger than resonance III at point C, the nonlinear frequency broadening will be boosted again towards an ultra-wide resonance at point F. Such frequency broadening behavior is the hybrid effect of nonlinear and multi-frequency mechanisms. It should be noted that the multi-frequency mechanism should be designed with a proper frequency interval, such that the nonlinear shifted resonance is capable of stepping over its following resonance at a certain ambient excitation.

The packaged energy harvesting device with HFB mechanism is tested by a closed-loop vibration control system. It is capable of providing a frequency sweep-sine within a specific frequency range at constant vibration acceleration. Fig. 4(a) shows the experimental results of the output voltages against frequency up-sweep and down-sweep within a range of 50–150 Hz at a low acceleration of 0.1g. It is seen from the down-sweep spectrum that the first two resonance peaks occur at 62.9 and 82.1 Hz, which is in good agreement with the simulation results. From the up-sweep voltage spectrum, a strong nonlinear behavior is observed due to the hybrid nonlinear effect of modes I and II. Comparing with the down-sweep voltage peaks of 0.01 mV at 62.9 Hz and 0.013 mV at 82.1 Hz, the voltage peak is enhanced to be 0.051 mV at a broadened resonance of 114.8 Hz. Fig. 4(b) shows the voltage response for frequency up-sweep at accelerations of 0.2g, 0.4g, 0.6g, and 1.0g. At the acceleration of 0.2g, the nonlinear frequency broadening effect continues, and the shifted resonant peak is 0.067 mV at 139.7 Hz, which is approach to resonance mode III. As the acceleration changes to 0.4g, the steadily increased bandwidth exceeds the resonance mode III of 150 Hz, and a further simulated nonlinear effect occurs. As a result, the resonance is further extended from 139.7 to 304.7 Hz with an ultra-wide frequency span of 165 Hz. Afterwards, the HFB effect enables its resonance to shift towards higher frequencies of 344.9 and 383.7 Hz with voltage outputs of 0.275 and 0.339 mV, respectively, at the accelerations of 0.6g and 1.0g.

From the above experimental results, it is concluded that the proposed device with HFB mechanism can gain a bandwidth enhancement from its original resonance of 62.9 Hz up to the widest nonlinear resonance of 383.7 Hz at 1.0g. The strong nonlinear behavior is due to the hybrid effect of Duffing stiffening of the clamped-clamped beam stretching at three distributed resonances, which are out-of-plane mode I at 62.9 Hz, torsion mode II at 82.1 Hz, and twist mode III at 150 Hz. This work offers a promising design methodology of ultra-wideband MEMS energy harvesting for adapting a wide range of vibration scenarios.

This work was partially supported by Faculty Research Committee (FRC) Grant No. (R-263-000-692-112) at the National University of Singapore (NUS), the NRF-CRP001-057 Program "Self-powered body sensor network for disease management and prevention-oriented healthcare" under R-263-000-A27-281 from National Research Foundation (NRF), Singapore, and the doctoral program of higher education special fund project, China (Grant No. 20133201130003).

[1]S. P. Beeby, M. J. Tudor, and N. M. White, Meas. Sci. Technol. **17**(12), R175–R195 (2006).
[2]D. B. Zhu, M. J. Tudor, and S. P. Beeby, Meas. Sci. Technol. **21**(2), 022001 (2010).
[3]H. Liu, C. Lee, T. Kobayashi, C. J. Tay, and C. Quan, Smart Mater. Struct. **21**(3), 035005 (2012).
[4]H. Liu, C. J. Tay, C. G. Quan, T. Kobayashi, and C. Lee, J. Microelectromech. Syst. **20**(5), 1131–1142 (2011).
[5]L. G. W. Tvedt, D. S. Nguyen, and E. Halvorsen, J. Microelectromech. Syst. **19**(2), 305–316 (2010).
[6]S. D. Nguyen, E. Halvorsen, and I. Paprotny, Appl. Phys. Lett. **102**(2), 023904 (2013).
[7]B. Marinkovic and H. Koser, Appl. Phys. Lett. **94**(10), 103505 (2009).
[8]A. Hajati and S.-G. Kim, Appl. Phys. Lett. **99**(8), 083105 (2011).
[9]B. Yang, C. Lee, W. Xiang, J. Xie, J. H. He, R. K. Kotlanka, S. P. Low, and H. Feng, J. Micromech. Microeng. **19**(3), 035001 (2009).
[10]H. Liu, Y. Qian, and C. Lee, Sens. Actuators, A **204**, 37–43 (2013).
[11]H. Liu, B. W. Soon, N. Wang, C. J. Tay, C. Quan, and C. Lee, J. Micromech. Microeng. **22**(12), 125020 (2012).
[12]S. D. Senturia, *Microsystem Design* (Springer, New York, 2004), pp. 249–252.